were completely abolished within a week of the *Bckdk*$^{-/-}$ mice starting the BCAA-enriched diet, which suggests that they have an inducible yet reversible phenotype (Fig. 3C).

Our experiments have identified a Mendelian form of autism with comorbid ID and epilepsy that is associated with low plasma BCAAs. Although the incidence of this disease among patients with autism and epilepsy remains to be determined, it is probably quite a rare cause of this condition. We have shown that murine *Bckdk*$^{-/-}$ brain has a disrupted amino acid profile, suggesting a role for the BBB in the pathophysiology of this disorder. The mechanism by which abnormal brain amino acid levels lead to autism, ID, and epilepsy remains to be investigated. We have shown that dietary supplementation with BCAAs reverses some of the neurological phenotypes in mice. Finally, by supplementing the diet of human cases with BCAAs, we have been able to normalize their plasma BCAA levels (table S10), which suggests that it may be possible to treat patients with mutations in *BCKDK* with BCAA supplementation.

References and Notes

1. R. Tuchman, I. Rapin, *Lancet Neurol.* **1**, 352 (2002).
2. A. Bailey *et al*., *Psychol. Med.* **25**, 63 (1995).
3. D. Seelow, M. Schuelke, F. Hildebrandt, P. Nürnberg, *Nucleic Acids Res.* **37** (Web Server issue), W593 (2009).
4. M. Machius, J. L. Chuang, R. M. Wynn, D. R. Tomchick, D. T. Chuang, *Proc. Natl. Acad. Sci. U.S.A.* **98**, 11218 (2001).
5. R. A. Harris, M. Joshi, N. H. Jeoung, M. Obayashi, *J. Nutr.* **135** (suppl.), 1527S (2005).
6. A. Suryawan *et al*., *Am. J. Clin. Nutr.* **68**, 72 (1998).
7. J. H. Menkes, P. L. Hurst, J. M. Craig, *Pediatrics* **14**, 462 (1954).
8. S. E. Snyderman, P. M. Norton, E. Roitman, L. E. Holt Jr., *Pediatrics* **34**, 454 (1964).
9. C. B. Doering, C. Coursey, W. Spangler, D. J. Danner, *Gene* **212**, 213 (1998).
10. C. J. Lynch *et al*., *Am. J. Physiol. Endocrinol. Metab.* **285**, E854 (2003).
11. M. A. Joshi *et al*., *Biochem. J.* **400**, 153 (2006).
12. N. Lepage, N. McDonald, L. Dallaire, M. Lambert, *Clin. Chem.* **43**, 2397 (1997).
13. K. Okita *et al*., *Nat. Methods* **8**, 409 (2011).
14. S. H. Yuan *et al*., *PLoS ONE* **6**, e17540 (2011).
15. H. T. Chao *et al*., *Nature* **468**, 263 (2010).
16. M. J. Schmeisser *et al*., *Nature* **486**, 256 (2012).
17. R. A. Hawkins, R. L. O'Kane, I. A. Simpson, J. R. Viña, *J. Nutr.* **136** (suppl.), 218S (2006).
18. R. Duelli, B. E. Enerson, D. Z. Gerhart, L. R. Drewes, *J. Cereb. Blood Flow Metab.* **20**, 1557 (2000).
19. C. A. Wagner, F. Lang, S. Bröer, *Am. J. Physiol. Cell Physiol.* **281**, C1077 (2001).
20. F. Verrey, *Pflugers Arch.* **445**, 529 (2003).
21. W. J. Zinnanti *et al*., *Brain* **132**, 903 (2009).

Acknowledgments: We thank the families for their participation; R. Weavers and E. Morava (Nijmegen Medical Center, Netherlands) and B. Barshop for providing patients; M. Kara's colleague for arranging shipment during the Libyan revolution; C. Lynch for the pSer293 antibody; the S. Taylor lab (UCSD) for help in protein modeling; M. Seashore, W. MacLean Jr., T. Cowan, and A. El-Gharabawy for suggestions; N. Wright-Davis, M. Murtha, M. Raubeson, N. DiLullo, M. Walker, Y. Song, N. Lifton, K. Bilguvar, A. Caglayan, Z. Omay, M. Choi, N. Carriero, R.D. Bjornson, P. Ventola, K. Koenig, and A. Bozik for technical assistance; the Yale Center for Genome Analysis (S. Mane); and the Sanford Burnham Institute. Supported by NIH grants P01HD070494, R01NS048453, and P30NS047101 (J.G.G.), RC2MH089956 (M.W.S.), K08MH087639 (A.R.G.), T32MH018268 and (P.E.-F.); Broad Institute grant U54HG003067 (E.L.); the Center for Inherited Disease Research for genotyping; the Simons Foundation Autism Research Initiative (J.G.G. and M.W.S.); a Veterans Administration Merit Award (R.A.H.); the German Research Foundation (G.N.); the American Academy of Child and Adolescent Psychiatry Pilot Research Award/Elaine Schlosser Lewis Fund (P.E.-F.); and the American Psychiatric Association/Lilly Research Fellowship (P.E.-F.). J.G.G. is an investigator of the Howard Hughes Medical Institute. Data have been deposited into dbGap (phs000288) and the NCBI Sequence Read Archive (SRS351252) (whole exome sequencing) and into GEO (GSE39447) (microarrays). J.G.G. is a consultant for Halozyme Therapeutics, a biopharmaceutical company that develops products targeting the extracellular matrix. M.W.S. is a consultant to Synapdx, that is developing diagnostic tests for autism, and to Pfizer Pharmaceuticals that is working to develop autism therapeutics. *Bckdk* gene trap mice are available for noncommercial research from R.A.H. under MTA agreement with Lexicon. J.G.G. and M.W.S. are inventors on a patent application filed 17 July 2012 by UCSD covering diagnostic and therapeutic strategies for patients with autism and epilepsy.

Supplementary Materials

www.sciencemag.org/cgi/content/full/science.1224631/DC1
Materials and Methods
Supplementary Text
Figs. S1 to S10
Tables S1 to S10
References (*22*–*37*)

14 May 2012; accepted 8 August 2012
Published online 6 September 2012;
10.1126/science.1224631

Direct Observation of Cotranscriptional Folding in an Adenine Riboswitch

Kirsten L. Frieda[1] and Steven M. Block[2,3]*

Growing RNA chains fold cotranscriptionally as they are synthesized by RNA polymerase. Riboswitches, which regulate gene expression by adopting alternative RNA folds, are sensitive to cotranscriptional events. We developed an optical-trapping assay to follow the cotranscriptional folding of a nascent RNA and used it to monitor individual transcripts of the *pbuE* adenine riboswitch, visualizing distinct folding transitions. We report a particular folding signature for the riboswitch aptamer whose presence directs the gene-regulatory transcription outcome, and we measured the termination frequency as a function of adenine level and tension applied to the RNA. Our results demonstrate that the outcome is kinetically controlled. These experiments furnish a means to observe conformational switching in real time and enable the precise mapping of events during cotranscriptional folding.

Structured RNAs function during transcription or translation to influence a variety of processes. In vivo, nascent RNAs fold as they are transcribed, and this sequential process affects the folding efficiency (*1*–*4*) and the predominant conformation (*5*–*9*). The study of cotranscriptional folding has heretofore been largely indirect, with most approaches monitoring the final RNA product (*1*–*10*). Using single-molecule spectroscopy, we developed a system to visualize RNA folding in an individual, nascent transcript directly and used it to record the functional switching of a riboswitch. The conformation of the riboswitch ligand-binding aptamer affects the structure of the downstream RNA through changes in the availability of nucleotides shared between the aptamer and an "expression platform," which lead to structure-dependent gene regulation (*11*, *12*). The *pbuE* riboswitch from *Bacillus subtilis* regulates adenine levels, controlling transcription of downstream genes by forming an aptamer, which binds adenine and acts as an antiterminator, or an expression platform, consisting of a terminator hairpin that halts transcription (*13*) (Fig. 1A). Previous work has considered the posttranscriptional folding of this aptamer (*13*–*16*). Here, we consider the functional consequences of the aptamer and terminator domains acting in concert in real time. Following transcription of the full riboswitch, only the folded terminator has previously been observed (*15*–*18*), as expected, given the far greater energetic stability of this domain (*19*). Any switching behavior must therefore be studied in the context of active transcription.

In our assay (*14*, *20*), a transcriptionally stalled molecule of *Escherichia coli* RNA polymerase (RNAP) carrying a short initial transcript was tethered in a dual-beam optical tweezers apparatus in a "dumbbell" configuration (*19*), with RNAP linked to one bead and the transcript linked to the other via hybridization to a complementary, cohesive end of a dsDNA "handle" (*14*, *21*) (Fig. 1B). Transcription was restarted by the addition of nucleoside triphosphates (1 mM NTPs) in the presence or absence of saturating levels of adenine base

[1]Biophysics Program, Stanford University, Stanford, CA 94305, USA. [2]Department of Applied Physics, Stanford University, Stanford, CA 94305, USA. [3]Department of Biology, Stanford University, Stanford, CA 94305, USA.

*To whom correspondence should be addressed. E-mail: sblock@stanford.edu

(300 μM), and the separation between beads was measured. Transcription proceeded through the riboswitch, either finishing at the position of the terminator—where the dumbbell assembly dissociated as RNAP released the RNA—or continuing to the end of the template, where RNAP was arrested by a streptavidin roadblock—at which point the dumbbell tether remained intact (Fig. 1C).

Adenine-dependent termination was measured both in bulk (no force) and for single molecules (Fig. 2, A and B). Termination was scored as the termination efficiency (TE), defined as the fraction of complexes dissociating at the terminator position. Bulk assays gave high levels of termination in the absence of adenine (89%) that decreased in its presence (49%, for saturating adenine). For single molecules, the TE depends force, because folded conformations of the aptamer and terminator are destabilized by increasing loads. At low forces, where these structures can form (<7 pN), TEs were similar to those in bulk. Without adenine (Fig. 2B, blue), most transcripts terminated at low force, but TEs decreased under loads approaching the unfolding force of the terminator hairpin (~13 pN). This behavior is identical to that reported for intrinsic terminators alone and fit by a quantitative model (*19*, *21*). The upstream aptamer sequence in the absence of adenine only slightly lowered the TE (at $F = 0$) relative to that of the isolated terminator. Under saturating adenine levels (Fig. 2B, red), the TE remained near 50% throughout the low-force regime, where the aptamer folds readily, but defaulted to the identical load dependence as data acquired without adenine for forces beyond ~7 pN, the equilibrium value for folding of the aptamer region alone. These results imply that, absent an adenine-reinforced aptamer caused by either (i) a lack of adenine or (ii) a load-dependent destabilization of the aptamer, the riboswitch behaves as an unhindered terminator.

We observed transcription directly, including cotranscriptional folding events, by monitoring transcript extension change over time. By shortening RNA tethers into the range of hundreds of bases, which increases stiffness and reduces noise, and lowering the tension below levels sufficient to open short hairpins, we were able to visualize structure formation as it took place. We also revised our protocols to measure transcription without significant delay from the restart of transcription (*19*). Two antagonistic effects control end-to-end transcript length: The extension tends to increase overall as RNA gets synthesized but may decrease whenever the nascent chain folds. An illustration of such lengthening is found in Fig. 2C, as the first part of the stem and the loop of a simple hairpin are synthesized. This phase is followed by shortening as the complementary portion of the stem is generated, until the folding completes, whereupon lengthening resumes until the roadblock is reached.

In transcription records of the adenine riboswitch obtained at comparatively high loads ($F =$

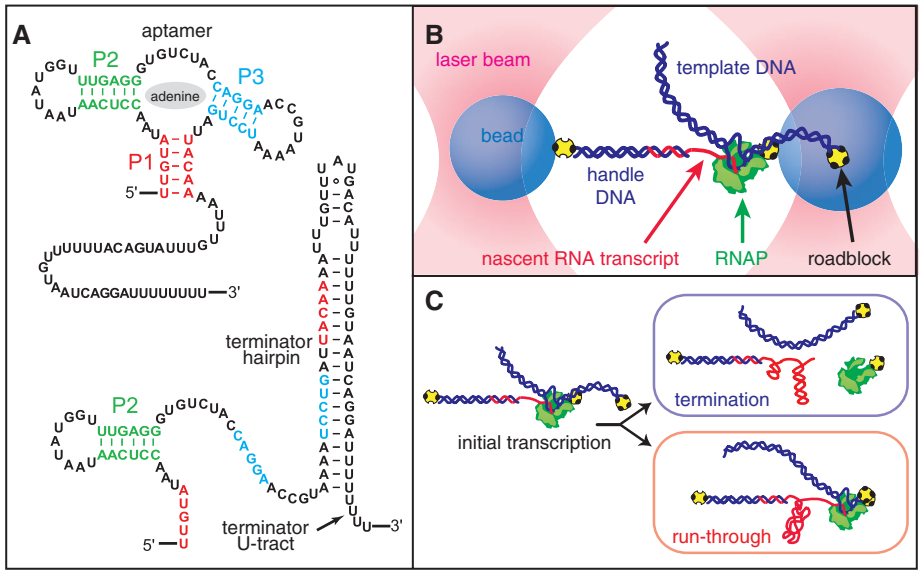

Fig. 1. (**A**) Secondary structure of competing aptamer and terminator conformations of the *pbuE* riboswitch. (**B**) Schematic of the "dumbbell" assay showing the experimental geometry, with the nascent RNA transcript transcribed in situ (not to scale). (**C**) Elongation produces the riboswitch, causing RNAP to dissociate at the terminator element or to run through to the roadblock at the template end.

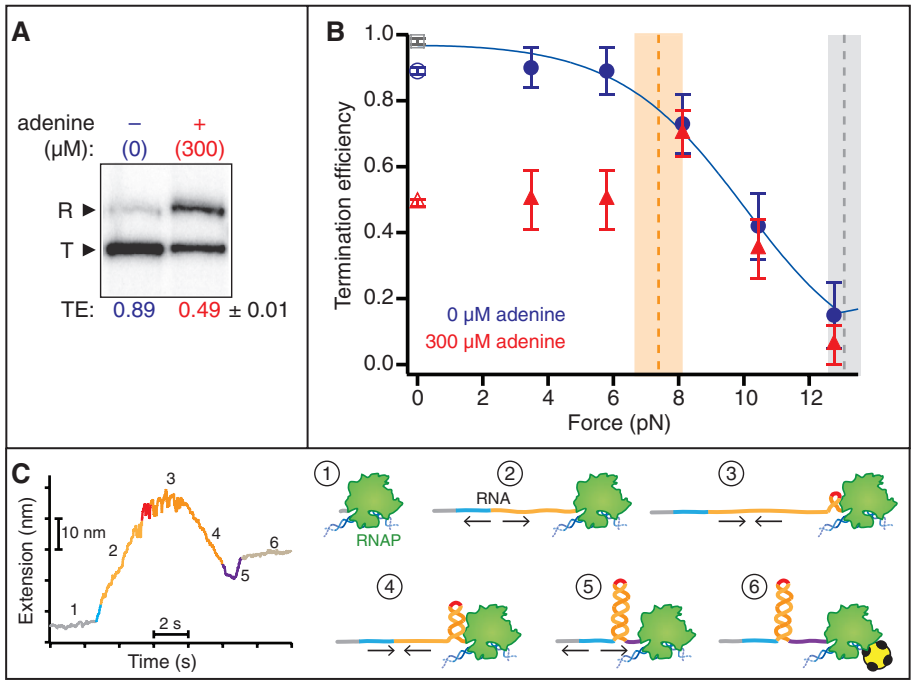

Fig. 2. Termination efficiency (means ± SEM). (**A**) TE from a gel-based assay with termination (T) and run-through (R) bands, and (**B**) as a function of tension applied to the RNA. Data under load were from single-molecule records (filled symbols); zero-force points were from gel assays (open symbols). Blocking RNA upstream of the terminator with a DNA oligomer suppressed aptamer formation and created an isolated terminator, raising TE slightly (gray open square). Data without adenine were fit by a model of intrinsic termination (blue curve). The equilibrium unfolding forces of the adenine-bound aptamer and terminator hairpin are indicated (orange, gray shading and dashed lines, respectively; means ± SD). (**C**) Cotranscriptional folding of a hairpin (left; 72 base pairs, 12 pN load). Stages during transcription are illustrated (right; not to scale): (1) Extension remains constant before transcription restart, then (2) increases (outward arrows) during elongation until (3) the duplex nucleates, causing extension to decrease (inward arrows) as (4) the hairpin forms. Once the hairpin is completed, (5) elongation resumes until RNAP reaches the roadblock (6).

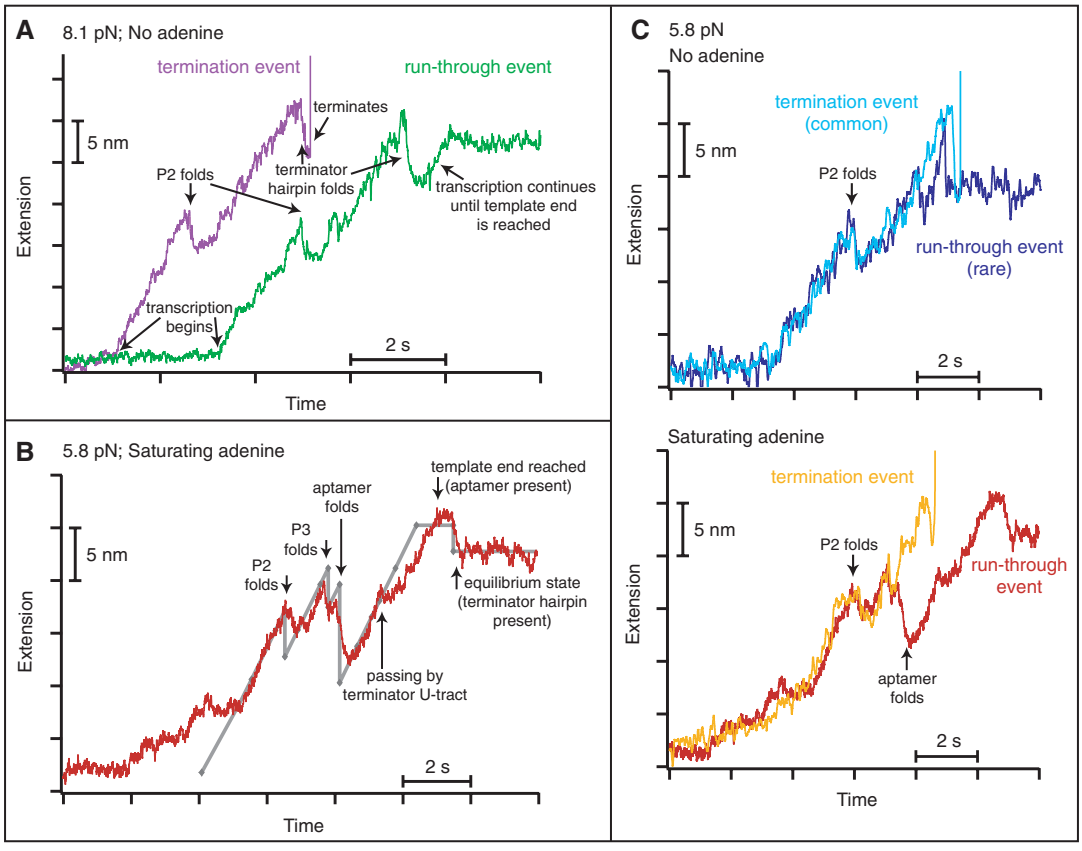

Fig. 3. Riboswitch transcription showing cotranscriptional folding. Transcript extension generally increased during transcription, with local decreases induced by folding events. Terminating traces led to RNA release and a sharp upward displacement, corresponding to tether breakage; run-through traces remained at a fixed extension once RNAP encountered the terminal roadblock. Records were collected in 0 μM or 300 μM adenine (saturating). (**A**) At high forces, where the aptamer rarely folds (8.1 pN), folding is adenine-independent (fig. S3); there is no outcome-correlated difference in folding patterns (purple versus green traces). Records are offset for display. (**B**) At lower forces (5.8 pN), run-through traces displayed the characteristic signature of bound aptamer formation. A run-through record is superimposed against a simple folding model (gray; see supplementary materials), with the events indicated. (**C**) Records displayed distinct motifs correlated with the transcription outcome. Records overlaid: absent adenine (top), run-through events were rare and records did not display an aptamer folding signature following P2 formation, appearing indistinguishable from terminating records. With adenine (bottom), aptamer folding led to transcriptional run-through.

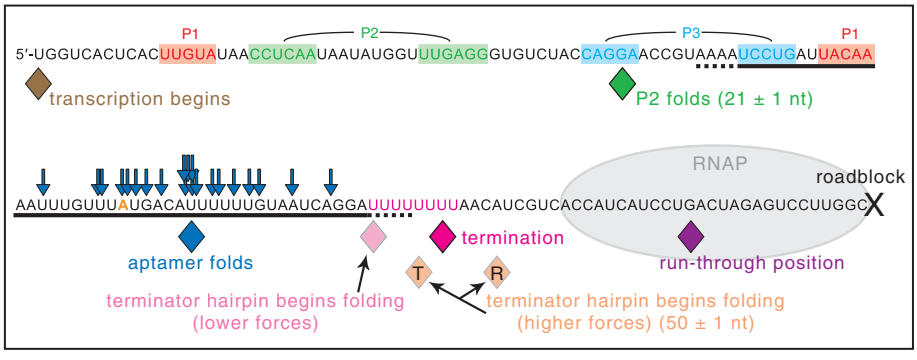

Fig. 4. Map of cotranscriptional folding events. The average computed position of the last nucleotide transcribed at the specified event is indicated (solid diamonds; SEM ± ~1 nt, approximately equal to the symbol width), beginning with the resumption of transcription at the 5′-U, ending with termination or run-through and roadblock arrest. The numbers of nucleotides associated with folding elements are indicated. Adenine-bound aptamer folding (blue diamond, average position; blue arrows, sampled individual observations) occurred between P1 and complete terminator transcription. For forces below 9 pN (5.8 pN, 8.1 pN), the terminator hairpin (underlined) was observed to begin folding (light pink diamond) before the termination position (dark pink diamond; transcript release). At higher forces (10.4 pN), the average folding position differed between traces that terminated (T, orange diamond) or ran through (R, orange diamond), occurring too late in the latter to produce successful termination. See table S2 for additional details.

8.1 pN) (Fig. 3A), extension increased monotonically during the synthesis of the early, unstructured sequence, followed by a decrease at the first fold, corresponding to the folding of the P2 stem-loop. Transcription continued until the terminator was reached, at which point its hairpin folded and transcription was terminated (releasing the RNA) or RNAP ran through to the end of the template. At this high force, the aptamer rarely forms, so the TEs and shapes of records were similar in the presence or absence of adenine (Fig. 3A and fig. S3).

At lower loads, adenine-dependent folding occurred in a way that decided transcriptional fate. The signature of aptamer folding appeared as a relatively large decrease in extension, after P2 folded and before the terminator hairpin was generated: This resulted in a stable fold, during which other folding events were not observed. A simplified model of cotranscriptional folding serves as a useful guide to track the folding events (Fig. 3B). P2 folded first, followed closely by P3 and then the aptamer. With the aptamer formed, RNAP is able to transcribe past the terminator hairpin without its folding. However, even in such cases, the adenine-bound aptamer was eventually observed to unfold and to be replaced by an equilibrium structure with the terminator hairpin folded. However, because RNAP had already moved beyond the terminator position, the RNA was not released.

Comparisons at lower force (5.8 pN) showed that in the presence of adenine, the vast majority of records destined to run through displayed a distinct folding signature, attributable to aptamer folding. Aptamer folding signatures were not observed in records that ultimately terminated or in rare run-through records obtained without adenine (Fig. 3C and fig. S4). With adenine present, the chance of run-through in a record carrying

the aptamer-folding signature was at least 95%. Conversely, the probability of transcriptional termination when the aptamer-fold signature was not scored but adenine was present was ~85%. The probability of run-through under such conditions (~15%) agrees closely with the probability of run-through in the absence of adenine.

On the basis of the short time window for folding and possible adenine binding in the *pbuE* aptamer before the termination decision (~2 s), and on the relatively long lifetime of the adenine-bound aptamer (~10 s) (*16*, *19*), as well as the dependence of TE on transcription rate (*18*), it has been conjectured that kinetic (as opposed to thermodynamic) effects would play a dominant role in controlling transcriptional fate. We find unambiguous evidence that the *pbuE* riboswitch is kinetically controlled, because aptamers were observed to fold and bind adenine once, or not at all, precluding any possible thermodynamic equilibration between conformations during the binding window, as transcription proceeded rapidly [~20 nucleotides (nt)/s]. Once formed, the adenine-bound aptamer rarely unfolded before the termination decision (fig. S5A), and it was observed to fold multiple times only in one unusually slow record (fig. S5B). The probability of forming an unproductive, aptamer-like fold (i.e., where the aptamer folds and unfolds at least once before influencing the outcome) is therefore low: 5% or fewer transcripts generated an unproductive, adenine-associated fold.

The flavin mononucleotide (FMN) riboswitch sequence contains two pause sites thought to be important for allowing FMN additional time to bind (*7*) and, possibly, increasing the time window for folding. In the *pbuE* riboswitch, two short series of uridine (U) residues, situated before the poly(U) tract of the terminator, have similarly been proposed to act as pause sites (*16*), with pausing reported in one of these regions, but only observed under limiting NTP conditions (*18*). In our experiments using physiological levels of NTPs, long pauses were not observed at either of these sites; pauses, if any, were too brief to identify (<1 s). This discrepancy might be attributed to the differences in NTP concentrations, to transcription by the cognate *B. subtilis* RNAP (although this is unlikely to increase pausing), or to the involvement of other factors (*7*, *18*, *22*), as discussed (*19*).

Our data show that the folded aptamer can persist briefly after transcription of the terminator hairpin, temporarily trapping the riboswitch far from equilibrium. Taking U8 of the terminator U tract as the position where the terminator is largely completed, we find that in the presence of adenine, run-through records unfolded beyond this point with a dwell time averaging 2.6 s (fig. S7). In the functional riboswitch, the aptamer persisted for a shorter time than it would have without any competing structure (~10 s for the adenine-bound aptamer) (fig. S7B), which implies that some mechanism—for example, branch migration—may facilitate conversion between states (*5*, *6*). The unfolding aptamer gave way to the terminator conformation instantaneously on the time scale of our apparatus (~50 ms), and the RNA remained thereafter in this equilibrium state (fig. S6).

Using data collected over a range of forces in the presence and absence of adenine, we can construct a map of cotranscriptional folding (Fig. 4 and table S2). P2 is the first significant structure to fold, sequestering 21 ± 1 nt (as expected, based on sequence) once RNAP reached a position 12 ± 1 nt after the last nucleotide of P2 was transcribed, which agrees closely with the ~12-nt RNA footprint estimated for RNAP (*23*, *24*). The aptamer region is transcribed by nt 74, and it folded, on average, when RNAP reached nt 90 ± 1, soon after the RNAP footprint cleared the aptamer. At low forces, if the aptamer failed to fold, the terminator hairpin formed later in transcription, once a segment of its complementary RNA hairpin sequence became available. Termination subsequently occurred at nt 112 ± 1, around U7 of the U tract, which is typical for intrinsic terminators (*25*). Notably, at higher forces for records that terminated, the terminator hairpin folded at nt 110 ± 1, whereas for records that ran through, the terminator folded later, at nt 117 ± 1 (after transcription of the downstream U tract), which supported the notion that the energy of hairpin formation assists in releasing the RNA. For loads close to the unfolding force of the terminator, records showed no evidence of cotranscriptional hairpin folding, and the vast majority ran through. The few records that terminated appeared to do so at the "slippery" U tract (*21*). In all records that ran through, RNAP arrested at nt 134 ± 1, a position ~15 nt upstream of the roadblock, consistent with the downstream footprint of RNAP (*26*, *27*).

These experiments provide a real-time window into transcript formation and functional switching in a riboswitch. Cotranscriptional folding is fundamental to the action of the *pbuE* adenine riboswitch, which exerts its modulatory effects far from equilibrium. Once the aptamer sequence is formed, the adenine-bound aptamer is able to briefly lock down the riboswitch conformation until RNAP has successfully passed the termination signal. Conversely, if the ligand-bound aptamer fails to become stabilized by the time RNAP reaches the decision point, the terminator hairpin forms instead, which leads to prompt transcript release at the terminator U tract. Cotranscriptional folding events follow a sequential progression, with associated structures forming within seconds (or less) of the times that their sequences clear the RNAP footprint. Nascent transcript structures that get trapped out of equilibrium are later found to switch conformations nearly instantly. The sensitivity of this system to kinetic details therefore poses a serious challenge in the quest for synthetic mimics of riboswitches in a bioengineering context. The experimental approaches presented here provide the opportunity to explore the dynamics of cotranscriptional folding directly in a variety of RNA structures. We anticipate that force spectroscopy will become a useful tool in the study of cotranscriptional events and, possibly, cotranslational events as well.

References and Notes

1. S. L. Heilman-Miller, S. A. Woodson, *RNA* **9**, 722 (2003).
2. T. Pan, X. Fang, T. Sosnick, *J. Mol. Biol.* **286**, 721 (1999).
3. T. Pan, I. Artsimovitch, X. W. Fang, R. Landick, T. R. Sosnick, *Proc. Natl. Acad. Sci. U.S.A.* **96**, 9545 (1999).
4. T. N. Wong, T. R. Sosnick, T. Pan, *Proc. Natl. Acad. Sci. U.S.A.* **104**, 17995 (2007).
5. A. Xayaphoummine, V. Viasnoff, S. Harlepp, H. Isambert, *Nucleic Acids Res.* **35**, 614 (2007).
6. E. M. Mahen, P. Y. Watson, J. W. Cottrell, M. J. Fedor, *PLoS Biol.* **8**, e1000307 (2010).
7. J. K. Wickiser, W. C. Winkler, R. R. Breaker, D. M. Crothers, *Mol. Cell* **18**, 49 (2005).
8. G. Nechooshtan, M. Elgrably-Weiss, A. Sheaffer, E. Westhof, S. Altuvia, *Genes Dev.* **23**, 2650 (2009).
9. G. A. Perdrizet 2nd, I. Artsimovitch, R. Furman, T. R. Sosnick, T. Pan, *Proc. Natl. Acad. Sci. U.S.A.* **109**, 3323 (2012).
10. T. Pan, T. Sosnick, *Annu. Rev. Biophys. Biomol. Struct.* **35**, 161 (2006).
11. T. M. Henkin, *Genes Dev.* **22**, 3383 (2008).
12. A. Roth, R. R. Breaker, *Annu. Rev. Biochem.* **78**, 305 (2009).
13. M. Mandal, R. R. Breaker, *Nat. Struct. Mol. Biol.* **11**, 29 (2004).
14. W. J. Greenleaf, K. L. Frieda, D. A. N. Foster, M. T. Woodside, S. M. Block, *Science* **319**, 630 (2008).
15. J. F. Lemay, J. C. Penedo, R. Tremblay, D. M. J. Lilley, D. A. Lafontaine, *Chem. Biol.* **13**, 857 (2006).
16. J. K. Wickiser, M. T. Cheah, R. R. Breaker, D. M. Crothers, *Biochemistry* **44**, 13404 (2005).
17. R. Rieder, K. Lang, D. Graber, R. Micura, *ChemBioChem* **8**, 896 (2007).
18. J. F. Lemay *et al.*, *PLoS Genet.* **7**, e1001278 (2011).
19. Materials and methods are available as supplementary materials on *Science* Online.
20. R. V. Dalal *et al.*, *Mol. Cell* **23**, 231 (2006).
21. M. H. Larson, W. J. Greenleaf, R. Landick, S. M. Block, *Cell* **132**, 971 (2008).
22. I. Artsimovitch, V. Svetlov, L. Anthony, R. R. Burgess, R. Landick, *J. Bacteriol.* **182**, 6027 (2000).
23. J. A. Monforte, J. D. Kahn, J. E. Hearst, *Biochemistry* **29**, 7882 (1990).
24. N. Komissarova, M. Kashlev, *Proc. Natl. Acad. Sci. U.S.A.* **95**, 14699 (1998).
25. Y. d'Aubenton Carafa, E. Brody, C. Thermes, *J. Mol. Biol.* **216**, 835 (1990).
26. S. A. Darst, *Curr. Opin. Struct. Biol.* **11**, 155 (2001).
27. S. J. Greive, P. H. von Hippel, *Nat. Rev. Mol. Cell Biol.* **6**, 221 (2005).

Acknowledgments: We thank R. Landick for providing purified RNAP and C. García-García, V. Schweikhard, W. Greenleaf, P. Anthony, and other members of the Block lab for useful discussions. The data described in this manuscript are tabulated in the main paper and in the supplementary materials. This research was supported by a grant from the National Institute of General Medical Services, NIH (S.M.B.), and an NSF Graduate Research Fellowship and Stanford Graduate Fellowship (K.L.F.).

Supplementary Materials

www.sciencemag.org/cgi/content/full/338/6105/397/DC1
Materials and Methods
Figs. S1 to S7
Tables S1 and S2
References (*28*–*34*)

6 June 2012; accepted 24 August 2012
10.1126/science.1225722

Direct Observation of Cotranscriptional Folding in an Adenine Riboswitch

Kirsten L. Frieda and Steven M. Block

Science, **338** (6105), .
DOI: 10.1126/science.1225722

Making a Riboswitch

During RNA synthesis by RNA polymerase (RNAP), nascent RNA will start to fold. This cotranscriptional folding can affect the final conformation and the function of the full-length RNA. Using single-molecule spectroscopy and optical tweezers, Frieda and Block (p. 397) followed the cotranscriptional folding of the *pbuE* riboswitch from *Bacillus subtilis* directly in real time, observing the formation of the adenine-binding aptamer structure or the alternative transcription terminator hairpin structure. The structures formed within seconds of their sequences clearing the RNAP footprint, confirming that the *pbuE* riboswitch is kinetically controlled.